

Influence of Donor Moiety in Ruthenium Sensitizers on the Properties of Dye-Sensitized Solar Cells

Hong-Minh Nguyen¹, Jongwan Choi¹, Ji Hyun Heo¹, Jin-Woo Oh¹,
Duc-Nghia Nguyen², and Nakjoong Kim^{1,*}

¹Department of Chemistry and Research Institute for Natural Science, Hanyang University,
17-Haengdang-Dong, Seongdong-gu, Seoul 133-791, Korea

²Polymer Division, Institute of Chemistry Vietnam Academy of Science and Technology,
18-Hoang Quoc Viet, Cau Giay, Hanoi, Vietnam

Heteroleptic ruthenium complexes $cis\text{-}[\text{Ru}(\text{H}_2\text{dcbpy})(\text{L})(\text{NCS})_2]$, where H_2dcbpy is 4,4'-dicarboxylic acid-2,2'-bipyridine and L is 4-(4-(N,N-di-(p-hexyloxyphenyl)-amino)styryl)-4'-methyl-2,2'-bipyridine (Rut-A) or 4-(4-(3,6-dihexyloxycarbazole-9-yl)-styryl)-4'-methyl-2,2'-bipyridine (Rut-B), have been synthesized and characterized by NMR, UV-Vis spectroscopy, and cyclic voltammogram. The effect of different electron donors on the properties of dye-sensitized solar cells has been studied. The power conversion efficiency of DSSC based on Rut-B is 6.1% while Rut-A delivered a lower efficiency of 4.52% under the same device fabrication and measuring conditions. The better photovoltaic performance of Rut-B is mainly associated with enhanced dye absorptivity and charge recombination suppression.

Keywords: Dye-Sensitized Solar Cells, Ruthenium Complexes, Conjugated Ligand, HOMO–LUMO Energy Level, Substituted Carbazole.

1. INTRODUCTION

Dye-sensitized solar cells (DSSCs) have attracted great attention due to their low-cost production and high efficiency (η).¹ In a DSSC, the photosensitive dye plays a crucial role because it can absorb visible light and injects the photoexcited electrons to the conduction band of metal oxide semiconductors (anatase TiO_2 , ZnO). Up to now, DSSCs based on ruthenium polypyridyl complex photosensitizers have exhibited the highest power conversion efficiency (11%) and long-term stability.^{2–5}

However, one of the main drawbacks of ruthenium sensitizers is the relatively low molar extinction coefficient in the visible and near-IR wavelengths. In order to solve this problem, the ancillary ligand has been modified by extending its conjugation with electron-donating groups such as thiophene, bithiophene, and thienothiophene.^{6–8} As an electron-rich molecule with a planar fused-ring heterocycle, carbazole has been used as an electron donor in organic dyes.^{9–11} The DSSCs based on these dyes showed high photovoltaic performance (6–8.3%).

According to the above mentioned data, we have designed and synthesized a bipyridine ligand

functionalized by substituted carbazole moiety as a donor to extend the π conjugated system. Another ligand was synthesized where carbazole was replaced by a substituted diphenylamine moiety. These two ligands were employed as ancillary ligands in ruthenium complexes (Rut-A, Rut-B). We also studied the effect of dye molecular structures, especially the carbazole and diphenylamine moieties on the photophysical, electrochemical properties of dyes as well as solar cell performance.

2. EXPERIMENTAL DETAILS

2.1. Characterization of Dyes

¹H-NMR spectra were recorded on a Varian INOVA 400 MHz NMR spectrometer in CDCl_3 or (DMSO)- d_6 . ESI-MS was performed on a HP 1100 LC/MS with acetonitrile as solvent and FAB-MS on a JMS-700 HRMS. The UV-Vis absorption spectra of the dye solution were recorded on a Shimadzu UV-3101 PC spectrophotometer. Cyclic voltammogram (CV) was measured with a three-electrode electrochemical cell on a CHI610B electrochemical analyzer. A platinum working electrode, platinum counter electrode, and Ag/AgCl reference electrode were used. The supporting electrolyte was 0.1 M

*Author to whom correspondence should be addressed.

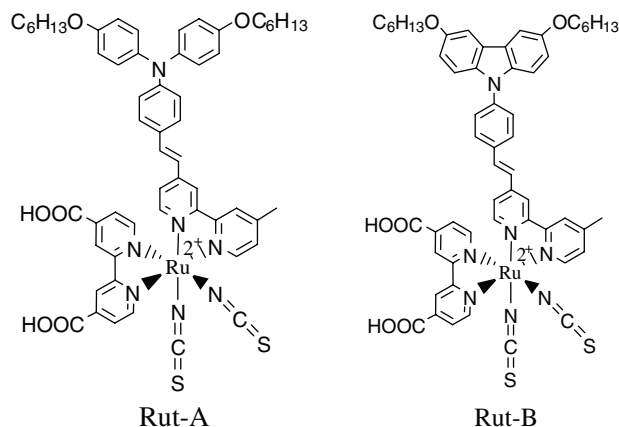
tetrabutylammonium tetrafluoroborate (Bu_4NBF_4) in acetonitrile and measurements were calibrated by the ferrocene/ferrocenium (Fc/Fc^+) couple potential.

2.2. Preparation and Measurement of Dye-Sensitized Solar Cells

Photoanodes of the DSSCs were prepared from a colloidal suspension of nanosized TiO_2 particles (Nanoxide-T, Solaronix, average size of 20 nm) by a doctor blade technique. The electrodes were sintered at 500 °C for 30 min in air to obtain TiO_2 films with thickness of 8 μm measured by a α -Step Profiler. These electrodes were immersed into solution containing 0.5 mM of ruthenium dyes for one day while still hot (80 °C). Solvents for the dye solution were $\text{CH}_3\text{CN}/t\text{-BuOH}$ (1:1 v/v) for Rut-A and Rut-B. Platinum-coated counter electrodes were obtained by spreading a drop of 5×10^{-3} M H_2PtCl_6 (Fluka) solution in isopropanol on the surface of a FTO glass and were treated in an oven at 400 °C for 15 min. The two electrodes were assembled using 25 μm thick Surlyn polymer (Dupont, 1702) and tightly held at 120–130 °C to seal the cell. The electrolyte was composed of 0.1 M lithium iodide, 0.1 M iodine, 0.5 M 4-*tert*-butylpyridine, and 0.6 M 1,2-dimethyl-3-propyl imidazolium iodide in acetonitrile. The photovoltaic characterization was carried out by illuminating the cell with a 1000 W Xenon lamp (Spectra-Physics) as a solar simulator. The light source was calibrated to 100 mW/cm^2 by a standard NREL Si solar cell equipped with a KG-5 filter to approximate AM 1.5G one sun light intensity. An active area of 0.32 cm^2 was irradiated. The current–voltage curves were obtained by measuring the photocurrent of the cell using a Keithley model 2400 digital source meter (Keithley, USA) under an applied external potential scan. Electrochemical impedance spectra (EIS) were measured by a frequency resonance analyzer (Solartron, SI 1260) connected to a potentiostat (Solartron 1287) with an oscillation level of 10 mV at the open-circuit voltage under 100 mV/cm^2 broadband illumination.

3. RESULTS AND DISCUSSION

The synthesis of 4-(4-(*N,N*-di(*p*-hexyloxyphenyl)amino)styryl)-4'-methyl-2,2'-bipyridine (ligand A) is based on the multi-steps synthetic pathway, starting from *N,N*-di-*p*-(hexyloxy)phenylamine. The carboxaldehyde intermediate was prepared by *N*-arylation of this amine with 4-bromobenzaldehyde. The synthesis of 4-(4'-(3,6-dihexyloxycarbazole-9-yl)styryl)-4'-methyl-2,2'-bipyridine (ligand B) is started from *N*-phenylcarbazole. This compound was converted to 3,6-dibromo-*N*-phenylcarbazole by bromination reaction with *N*-bromosuccinimide. This intermediate was followed by treatment with sodium and *n*-hexanol to afford 3,6-disubstituted phenylcarbazole. The Vilsmeier-Haack reaction was carried out to obtain



Scheme 1. Chemical structures of Rut-A and Rut-B sensitizers.

carboxaldehyde functional group. Two ligands were synthesized by two steps: nucleophilic addition of the anion of dimethylbipyridine with aldehyde intermediate, followed by dehydration of the corresponding alcohol in refluxing acetic acid. The synthesis of Ru(II) complexes was performed following a standard procedure developed by Grätzel and co-workers.¹² The target compounds were obtained in moderate yields and characterized by $^1\text{H-NMR}$ spectroscopy, mass spectrometry and were found to be consistent with the proposed structures as illustrated in Scheme 1.

The UV-Vis spectra of Rut-A and Rut-B dissolved in DMF (1×10^{-5} M) are shown in Figure 1 and the data are collected in Table I. The Rut-A sensitizer shows three maximum absorption peaks at 304 nm, 433 nm, and 526 nm. The band in UV region at 304 nm is assigned to the $\pi-\pi^*$ transition of bipyridine units. The second maximum at 433 nm is attributed to the $\pi-\pi^*$ transition of ligand A and one of the metal-to-ligand-charge transfer (MLCT) transition for Rut-A. The absorption band at

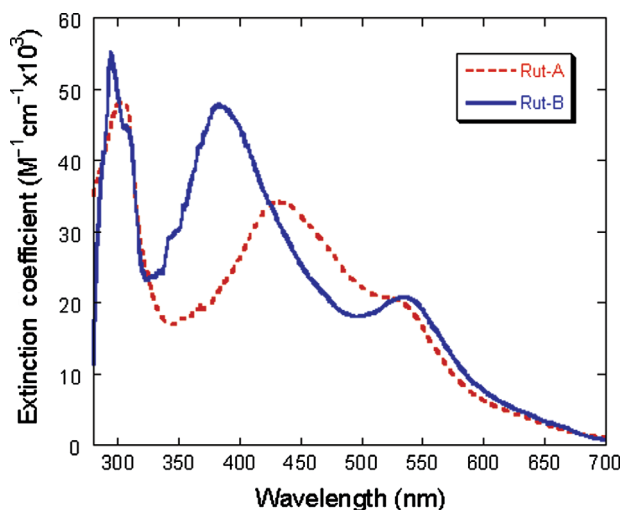


Fig. 1. Electronic absorption spectra of Rut-A and Rut-B in DMF.

Table I. Photophysical property and energy levels of Rut-A and Rut-B.

	Absorption $\lambda_{\text{MLCT}}/\text{nm}$ ($\epsilon \times 10^3 \text{ M}^{-1}\text{cm}^{-1}$)	V_{OX} (V vs. Ag/Ag ⁺)	HOMO ^a [eV]	LUMO [eV]	E_{gap}^b [eV]
Rut-A	526 (20.56)	0.78	-5.40	-3.32	2.08
Rut-B	535 (20.76)	0.87	-5.49	-3.41	2.08

^aHOMO was calculated from cyclic voltammogram. ^bBand gap was estimated from intersection of absorption and emission spectra in DMF.

526 nm corresponds to low energy MLCT caused by NCS ligands. Similar absorption bands can be observed for Rut-B with three bands at 294 nm, 384 nm, and 535 nm. The low energy MLCT absorption band of Rut-B exhibits high molar extinction coefficient of 20760 $\text{M}^{-1}\text{cm}^{-1}$, which is similar to that of Rut-A dye (20560 $\text{M}^{-1}\text{cm}^{-1}$) but the maximum is red shift by 9 nm compared to Rut-A, respectively. The enhanced molar extinction coefficient and the red-shift of MLCT band in Rut-B are due to the extension of the π -conjugation in hybrid sensitizer.

The cyclic voltammograms of Rut-A and Rut-B in DMF with 0.1 M tetrabutylammonium tetrafluoroborate show oxidation potentials at 0.78 V and 0.87 V versus Ag/Ag⁺ (Fig. 2), providing HOMO levels of -5.4 eV and -5.49 eV with respect to zero vacuum level. As summarized in Table I, the HOMO levels of Rut-A and Rut-B are calculated to be -3.32 eV and -3.41 eV, respectively, which are higher than the conduction band edge of TiO₂ (-4 eV, -0.5 V vs. NHE), ensuring the electron injection from excited dye molecules into the conduction band of TiO₂ is thermodynamically favorable. Both Rut-A and Rut-B show the same band gap (2.08 eV) but energy levels of Rut-B are shifted to more negative levels than those of Rut-A. This indicates that Rut-B dye incorporated carbazole moiety has lower energy levels than those for Rut-A with diphenylamine moiety.

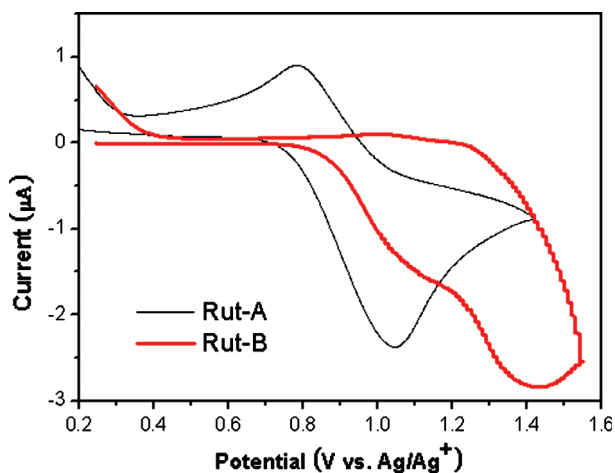


Fig. 2. Cyclic voltammograms of Rut-A and Rut-B in DMF: scanning rate is 50 mV/s; working electrode and counter electrode, Pt wires; reference electrode, Ag/AgCl.

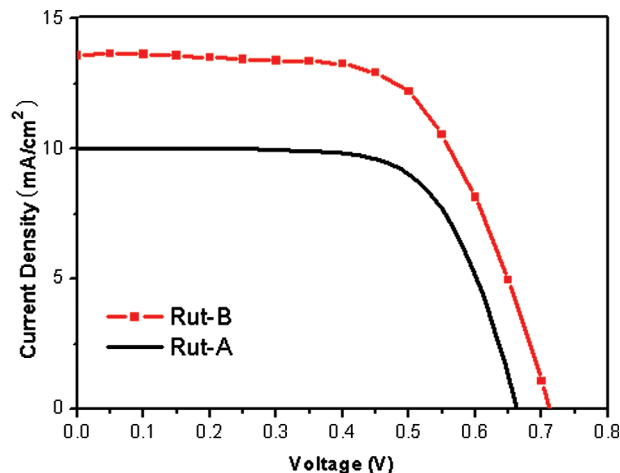
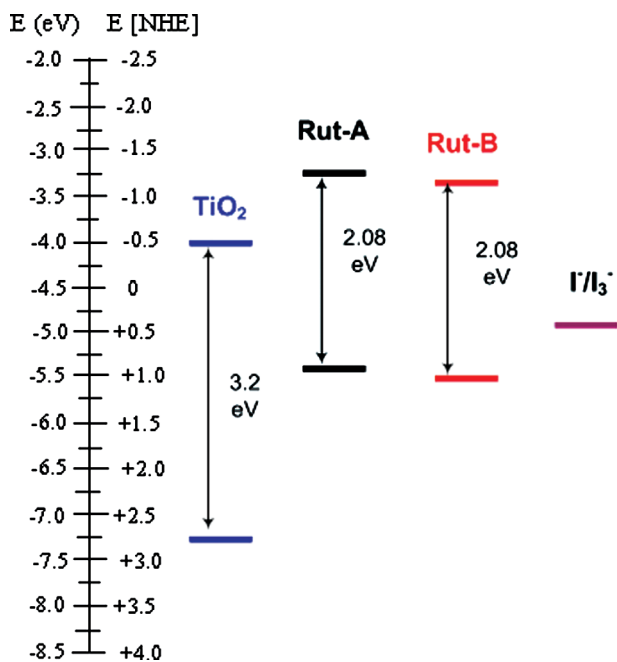


Fig. 3. Current density–voltage characteristics of DSSC devices with Rut-A and Rut-B as photosensitizers under AM 1.5G (100 mWcm^{-2}) illumination. (Thickness of TiO₂ film: 8 μm , active area: 0.32 cm^2).

The current density–voltage characteristics of the Rut-A and Rut-B sensitized cells are shown in Figure 3. Under standard global AM 1.5 solar irradiation, the short-circuit photocurrent density (J_{SC}), open-circuit voltage (V_{OC}) and fill factor (ff) of the device with Rut-A sensitizer are 10.04 mA/cm^2 , 0.662 V, and 0.68, respectively, corresponding to an overall conversion efficiency (η) of 4.52%. In contrast, the device based on Rut-B has a feature of higher J_{SC} (13.6 mA/cm^2) and V_{OC} (0.71 V) with a fill factor of 0.63, resulting in a higher η (6.1%) compared to Rut-A. This indicates that Rut-B with carbazole moiety as electron donor shows better performance compared to Rut-A. The higher J_{SC} value is contributed by Rut-B molar extinction coefficient with the enhanced absorptivity at long wavelengths. The HOMO level of Rut-A (-5.4 eV) is 0.09 eV higher than that of Rut-B (-5.49 eV) due to its lower oxidation potential, as illustrated in Scheme 2. This would lower the driving force for reduction of the oxidized dye by iodide anion. The lower dye regeneration efficiency is one of reasons for the lower conversion efficiency of Rut-A dye.

Electrochemical impedance spectroscopy (EIS) was performed under open-circuit-conditions and AM 1.5 simulated sunlight illumination (100 mW/cm^2). The results are displayed in the form of Nyquist plot, as shown in Figure 4. The Z_{real} and $-Z_{\text{img}}$ are the real part and imaginary part of the impedance, corresponding to the charge transfer resistant formed between interfaces and the resistant formed by the existence of electrochemical capacitance. In both DSSCs, total impedance of Rut-B/DSSC is higher than that of Rut-A/DSSC. The large semicircle at intermediate frequencies ($1-5 \times 10^2$ Hz) represents the electron transfer impedance at the TiO₂/dye/electrolyte interface. The charge transfer resistance at the TiO₂ surface (R_{CT2}) can be calculated by fitting curves from the range of intermediate frequencies using Z-view software. The



Scheme 2. Energy level diagram for Rut-A and Rut-B dyes.

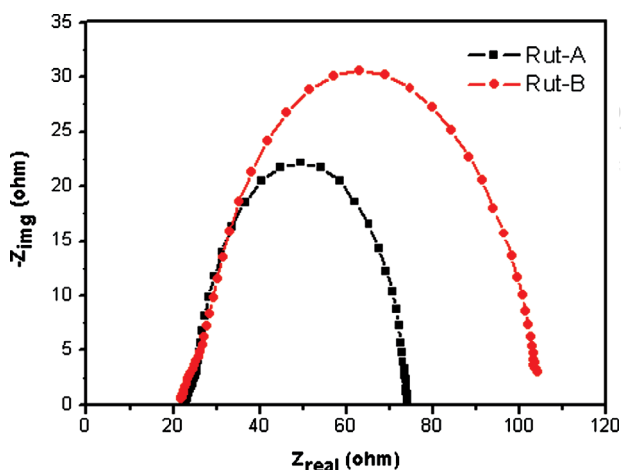


Fig. 4. Electrochemical impedance spectra (Nyquist plot) of DSSCs based on Rut-A and Rut-B dyes measured under open circuit conditions and AM 1.5 simulated sunlight illumination (100 mWcm^{-2}).

charge transfer resistance is related to the charge recombination rate. The R_{CT2} value for Rut-B was estimated to be 76 ohm that is larger than that for Rut-A (49 ohm), respectively, corresponding reduction in the radius of the semicircle. This impedance from the Rut-A dye-sensitized solar cell is evidence that the recombination process is faster than the Rut-B sensitizer, leading to the lower photovoltage of Rut-A dye cell. This indicates that incorporation of the substituted carbazole moiety in Rut-B decreases

effectively the probability of injected electron capture by electron acceptor (I_3^-) in the electrolyte.

4. CONCLUSION

In conclusion, two high molar extinction coefficient Ruthenium (II) complexes (Rut-A and Rut-B) carrying diphenylamine and carbazole moieties were synthesized and characterized. The introduction of carbazole moiety leads to red-shift of MLCT band and lower HOMO level of Rut-B dye compared to Rut-A. Incorporation of a substituted carbazole moiety in bipyridine ligand was demonstrated to be beneficial for retarding the electron transfer from TiO_2 to the oxidized dye or electrolyte and to enhance the charge transfer efficiency in the excited state, resulting in improved power conversion efficiency. Our future work is focused on the introduction of a new ancillary ligand containing one more substituted carbazole moiety to bathochromic shift the absorption and to control the energy levels of ruthenium complex.

Acknowledgment: This work was supported by the Korea Science and Engineering Foundation (KOSEF), Grant No. R11-2007-050-01003-0.

References and Notes

1. M. Grätzel, *Nature* 414, 334 (2001).
2. Y. Chiba, A. Islam, Y. Watanabe, R. Komiya, N. Koide, and L. Han, *Jpn. J. Appl. Phys.* 45, L638 (2006).
3. M. K. Nazeeruddin, F. D. Angelis, S. Fantacci, A. Selloni, G. Viscardi, P. Liska, S. Ito, B. Takeru, and M. Grätzel, *J. Am. Chem. Soc.* 127, 16835 (2005).
4. D. Kuang, P. Wang, S. Ito, S. M. Zakeeruddin, and M. Grätzel, *J. Am. Chem. Soc.* 128, 7732 (2006).
5. P. Wang, S. M. Zakeeruddin, J. E. Moser, M. K. Nazeeruddin, T. Sekiguchi, and M. Grätzel, *Nat. Mater.* 2, 402 (2003).
6. C. Y. Chen, S. J. Wu, C. G. Wu, J. G. Chen, and K. C. Ho, *Angew. Chem. Int. Ed.* 45, 5822 (2006).
7. F. Gao, Y. Wang, D. Shi, J. Zhang, M. Wang, X. Jing, R. H. Baker, P. Wang, S. M. Zakeeruddin, and M. Grätzel, *J. Am. Chem. Soc.* 130, 10720 (2008).
8. F. Gao, Y. Wang, J. Zhang, D. Shi, M. Wang, R. H. Baker, P. Wang, S. M. Zakeeruddin, and M. Grätzel, *Chem. Commun.* 23, 2635 (2008).
9. Z. S. Wang, N. Koumura, Y. Cui, M. Takahashi, H. Sekiguchi, A. Mori, T. Kubo, A. Furube, and K. Hara, *Chem. Mater.* 20, 3993 (2008).
10. Z. Ning, Q. Zhang, W. Wu, H. Pei, B. Liu, and H. Tian, *J. Org. Chem.* 73, 3791 (2008).
11. N. Koumura, Z. S. Wang, S. Mori, M. Miyashita, E. Suzuki, and K. Hara, *J. Am. Chem. Soc.* 128, 14256 (2006).
12. N. Hirata, J. J. Lagref, E. J. Palomares, J. R. Durrant, M. K. Nazeeruddin, M. Grätzel, and D. D. Censo, *Chem. Eur. J.* 10, 595 (2004).

Received: 31 October 2008. Accepted: 30 June 2009.